2016 International Conference on Applied Mathematics and Mechanics (ICAMM 2016)
ISBN: 978-1-60595-399-1

Stiffness Analysis of General Folding Frame of Mobile Solar Wing of Inverted Type

Ming-shi JI[1,*] and Yuan XUE[2]

[1]School of Mechatronics Engineering, Harbin Institute of Technology Harbin 150001, China

[2]School of Civil Engineering, Harbin Institute of Technology Harbin 150001, China

*Corresponding author

Keywords: Solar wing, Stiffness analysis, Folding frame.

Abstract. The simulation experiment on the solar wings, under the situation of zero gravity, is an important part of the satellite's ground work. With the development of space station and deep space exploration technology, the fold-expanding solar wing is being used more frequently, and there are higher requirements for its quality. As a result, the demand of the simulation experiment, which the solar wings worked on the ground with no gravity, also increase. In order to facilitate the comprehensive utilization of the test device, save space and improve the flexibility and speed of the test equipment, a new test device is provided, which is used for the unfoldment of mobile, retractable solar wings, working on the ground under zero gravity. In this paper, the calculation method for stiffness analysis is also given.

Introduction

With the development of the space station and deep detection technology, the fold expansion solar wing is using more frequently [1]. Higher requirements for its quality is put forward also, and the demand of its ground zero-gravity expand test is growing at the same time[2-3]. In order to facilitate utilization of the test device and save space, improve the flexibility and response speed of the test device, this paper presents a movable, scalable and automatic levelling solar wing ground zero gravity expand test device This device has the characters of high-precision, low friction, large span and large stiffness.

According to the technical requirements, the whole device uses the design of a two-stage hybrid telescopic lifting beam system seated by coarse adjustment and located by fine tune. The mechanical system of the device uses the spring and the strings system to solve the problem of the leveling and lock condition to eliminate the gap, which can provide a guarantee for the stability work of the system. This machinery uses a combination of rigid joint and hinge joint to solve the big span installation problem[4].

The structure of mobile solar wing unfolding device in Inverted type is shown as Figure 1.

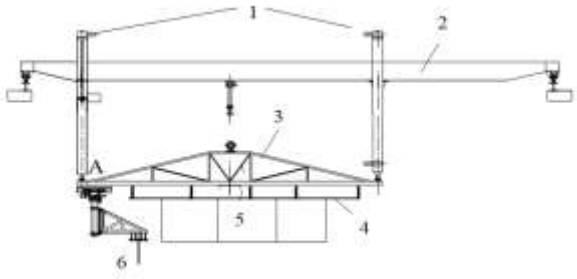

1- extending and retracting device, 2- Horizontally moving device, 3- Platform, 4- Rail device, 5- Solar wing

Figure 1. The inverted model.

Stiffness Analysis

The unfold shelf mechanical model is equivalent to the mechanical model shown in Figure 2.

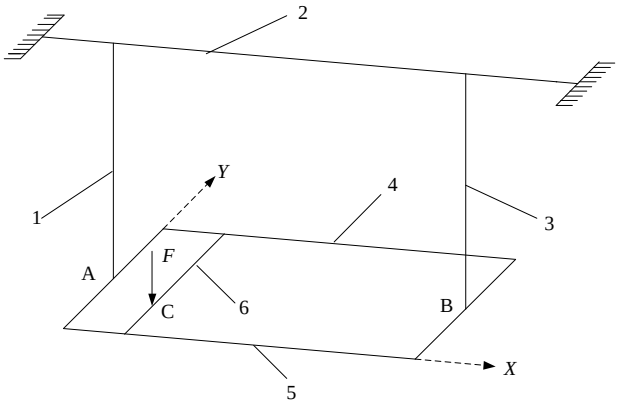

1-rod 3, 2-beam 5, 3-rod 4, 4-beam 2_2, 5-beam 2_1, 6-beam 1

Figure 2. The mechanical model.

Stiffness is mainly reflected as static stiffness [5]. According to the definition of stiffness, at any point on the transverse rail, the stiffness shows as

$$k = \frac{F}{\Delta x} \tag{1}$$

k, F and Δx, Respectively, stiffness, force and displacement.

Order F=1, and solve the deformation of any point, then the stiffness of this point is found out [5]. According to material deformation theory, deflection model of arbitrary simply supported beam is shown as Figure 3, deflection can be expressed as:

$$\begin{cases} \nu = -\dfrac{Fbx}{6EI_n}\left(l^2 - x^2 - b^2\right), \ 0 \le x \le a \\ \nu = -\dfrac{Fb}{6EI_n}\left[\dfrac{l}{b}\left(x-a\right)^3 + \left(l^2 - b^2\right)x - x^3\right], \ a \le x \le b \end{cases} \tag{2}$$

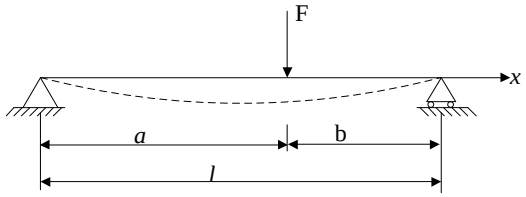

Figure 3. The deflection of beam under concentrated force.

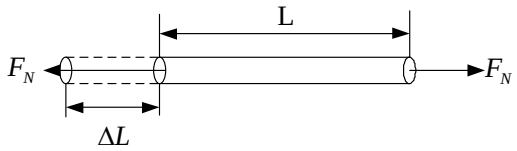

Figure 4. The axial tension rod deformation

For axial tension rod, Let its tensile strength as EA_m, A_m is the cross section area of the rod whose number is m. The deformation figure is shown as fig5. According to the axial tension rod deformation theory, the deflection can be solved as:

$$\Delta L = \frac{F_N L}{EA_m} \tag{3}$$

As to beam 1, its force is shown as Fig5. $a_1b_1 = y = \alpha_1 l_1, \ \alpha_1 + \beta_1 = 1$. According to the formula 1, the deflection of a_1 point is:

$$\nu_{a_1} = -\frac{F\beta_1^2\alpha_1^2 l_1^3}{3EI_1} \tag{4}$$

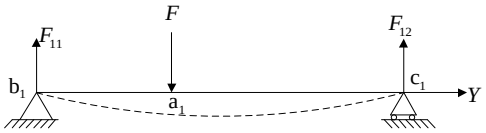

Figure 5. Force diagram of beam 1.

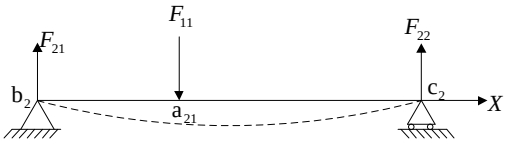

Figure 6. Force diagramof beam 2_1

Force diagram of beam 2_1 is shown as Fig.6, $a_{21}b_2 = x = \alpha_2 l_2$, $\alpha_2 + \beta_2 = 1$, when analogy with beam 1, the supporting force of beam 2_1 is $\begin{cases} F_{21} = \beta_2 F / 2 \\ F_{22} = \alpha_2 F / 2 \end{cases}$, and the deflection of a_{21} is :

$$\nu_{a_{21}} = -\frac{\beta_1 F \beta_2^2 \alpha_2^2 l_2^3}{3EI_2} \tag{5}$$

In the same way, the deflection of point a_{22}, which is on the beam 3 and is parallel to the beam 2, is:

$$\nu_{a_{22}} = -\frac{\alpha_1 F \beta_2^2 \alpha_2^2 l_2^3}{3EI_2} \tag{6}$$

According to static equilibrium, the axial tensions of rod 3 and 4 are: $\begin{cases} F_3 = \beta_2 F \\ F_4 = \alpha_2 F \end{cases}$, combining the formula (2) can obtain the axial deformation of the rod 3 and 4:

$$\Delta l_3 = \frac{F_3 l_3}{EA_3} = \frac{\beta_2 F l_3}{EA_3} \tag{7}$$

$$\Delta l_4 = \frac{F_4 l_4}{EA_4} = \frac{\alpha_2 F l_4}{EA_4} \tag{8}$$

As to beam 5, the force situation is shown as Fig.7. In order to the solve the deformations of point a_5 and d_5, let $a_5b_5 = \alpha_5 l_5$, $\alpha_5 + \beta_5 = 1$, $d_5b_5 = \alpha_6 l_5$, $\alpha_6 + \beta_6 = 1$, according to the superposition principle, the deformation of a_5 and d_5 are equal to the sum of deformation which F_3 and F_4 effect respectively[6].

In the separate effect of F_3, according to formula (1), the deflections of point a_5 and d_5 are:

$$\nu_{a_{51}} = -\frac{F_3 \beta_5^2 \alpha_5^2 l_5^3}{3EI_5} = -\frac{\beta_2 F \beta_5^2 \alpha_5^2 l_5^3}{3EI_5} \tag{9}$$

$$\nu_{d_{51}} = -\frac{F_3 \alpha_5 \beta_6 l_5^3}{6EI_5}\left(1 - \alpha_5^2 - \beta_6^2\right) = -\frac{\beta_2 F \alpha_5 \beta_6 l_5^3}{6EI_5}\left(1 - \alpha_5^2 - \beta_6^2\right) \tag{10}$$

In the separate effect of F_4, the deflections of point a_5 and d_5 are:

$$\nu_{a_{52}} = -\frac{F_4 \alpha_5 \beta_6 l_5^3}{6EI_5}\left(1 - \alpha_5^2 - \beta_6^2\right) = -\frac{\alpha_2 F \alpha_5 \beta_6 l_5^3}{6EI_5}\left(1 - \alpha_5^2 - \beta_6^2\right) \tag{11}$$

$$\nu_{d_{52}} = -\frac{F_4 \beta_6^2 \alpha_6^2 l_5^3}{3EI_5} = -\frac{\alpha_2 F \beta_6^2 \alpha_6^2 l_5^3}{3EI_5} \tag{12}$$

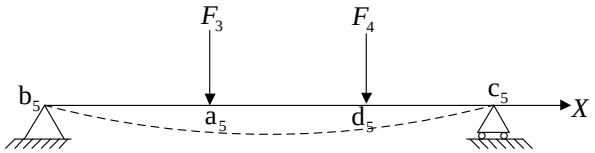

Figure 7. Force diagram of beam 5.

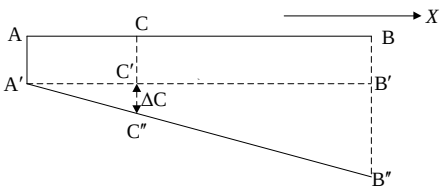

Figure 8. x direction geometry deformation of point C.

Combine with the formula (9) and (11), the deflection of point a_5 is:

$$\nu_{a_5} = \nu_{a_{51}} + \nu_{a_{52}} \tag{13}$$

Combine with the formula (10) and (12), the deflection of point d_5 is:

$$\nu_{d_5} = \nu_{d_{51}} + \nu_{d_{52}} \tag{14}$$

Combine with the formula (13), (14), (8) and (9), the displacements of point A and B are:

$$\Delta A = \nu_{a_5} + \Delta l_3 \tag{15}$$

$$\Delta B = \nu_{d_5} + \Delta l_4 \tag{16}$$

In X direction, as the displacements of point A and B are different, let $\Delta A < \Delta B$, according to the geometry relationship, there will be displacement at the point C[7], and the displacement is:

$$\Delta C_1 = \alpha_2 \left(\Delta B - \Delta A\right) == \alpha_2 \left(\nu_{d_5} + \Delta l_4 - \nu_{a_5} - \Delta l_3\right) \tag{17}$$

In the same way, in Y direction, let $\nu_{a_{21}} > \nu_{a_{22}}$, there will be displacement at the point C because of the different displacements of point a_{21} and a_{22}, and the displacement is:

$$\Delta C_2 = \alpha_2 \left(\nu_{a_{21}} - \nu_{a_{22}}\right) \tag{18}$$

From the above analysis, the total displacement of point C is:

$$\begin{aligned} x_C &= \nu_{a_1} + \nu_{a_{22}} + \nu_{a_5} + \Delta l_3 + \Delta C_1 + \Delta C_2 \\ &= F\frac{\beta_1^2\alpha_1^2 l_1^3}{3EI_1} + F\frac{2\alpha_1\beta_1\beta_2^2\alpha_2^2 l_2^3}{3EI_2} + F\frac{l_5^3}{3EI_5}\left(\beta_2^2\beta_5^2\alpha_5^2 + \alpha_2^2\alpha_6^2\beta_6^2\right) \\ &\quad + F\frac{\alpha_2\beta_2\alpha_5\beta_6 l_5^3}{3EI_5}\left(1-\alpha_5^2-\beta_6^2\right) + F\frac{\beta_2^2 l_3}{EA_3} + \frac{\alpha_2^2 l_4}{EA_4} \end{aligned} \tag{19}$$

Take $\alpha_1 = \frac{y}{l_1}, \beta_1 = 1 - \frac{y}{l_1}, \alpha_2 = \frac{x}{l_2}, \beta_2 = 1 - \frac{x}{l_2}$ into equation (1):

$$K\left(x,y\right) = \frac{1}{ax^2 + bx + my^4 - ny^3 + ky + c + f\left(x,y\right)} \tag{20}$$

When $y = \frac{l_1}{2}$:

$$K\left(x,y\right) = \frac{1}{ax^2 + bx + c + \frac{l_1^3}{48EI_1} + \frac{x^4}{6EI_2 l_2} - \frac{x^3}{3EI_2} + \frac{l_2}{6EI_2}x^2} \tag{21}$$

As $A=\frac{1}{6EI_2l_2}$, $B=\frac{1}{3EI_2}$, $C=\frac{l_2}{6EI_2}+a$, $D=b$, $F=c+\frac{l_1^3}{48EI_1}$, the equation (21) can be simplified as:

$$K(x,y)=\frac{1}{Ax^4-Bx^3+Cx^2+Dx+F} \tag{22}$$

Example Analysis

According to the structure model in Fig1, the data in design is:

$$\alpha_5=0.1,\ \beta_5=0.9,\ \alpha_6=0.6,\ \beta_6=0.4$$

$$l_1=0.04\text{m},\ R_1=0.05\text{m},\ l_2=10\text{m},\ l_3=l_4=6\text{m},\ l_5=20\text{m},\ R_2=R_3=R_4=R_5=0.25\text{m}$$

Take $x=2, F=1$ into equation (19), the displacement is $6.7\times10^{-8}m$, using the finite element method can get the result that the displacement of point C is $6.72\times10^{-8}m$. The deviation between two results is only 0.3%. When the rated load is 1000N, the displacement is $6.7\times10^{-5}m$, and this result can be suit to the requirement of experimental solar wings.

Above calculations showed that: the stiffness of mobile solar wing of inverted type meets the requirements of the experiment, and the formula derived is accurate.

Conclusion

(1) A new structure form of the folding frame of mobile solar wing of inverted type is proposed. This new device improve the utilization of space and the working efficiency.

(2) Unit strength is introduced, in this paper. According to the principle of superposition, the formula for stiffness calculation is deduced, which is accurate as the example shows.

(3) The new form of folding frame structure and the formula for stiffness calculation can be the basis for the design and analysis of this kind of mechanical device.

References

[1] X.Q. Chang, G.T. Zheng, Y.S. Fan, Z.W. Luo. Thermally Induced Vibration Analysis of Solar Array Based on the Hybrid Element Model[C]//6th International Symposium on Test and Measurement. 2005:2663~2668.

[2] Tang X, Hou J, Ni T, et al. Analysis on autonomous task trajectory tracking performance of construction robot with online gravity compensation [J]. Nongye Gongcheng Xuebao/Transactions of the Chinese Society of Agricultural Engineering, 2013, 29(3):30-37.

[3] Jagannathan S, Fenn R C, Johnson B G. Low-cost active anti-gravity suspension system[C]//American Control Conference, Proceedings of the 1995. IEEE, 1995, 5:3606-3611.

[4] Callens N, Ventura-Traveset J, De Lophem T-L, et al. ESA parabolic flights, drop tower and centrifuge opportunities for university students [J]. Microgravity Science and Technology, 2011, 23(2): 181-189.

[5] Chen C I, Chen Y T, Wu S C, et al. Experiment and simulation in design of the board-level drop testing tower apparatus [J]. Experimental Techniques, 2012, 36(2): 60-69.

[6] Nechyba M C, Xu Y. Human-robot cooperation in space: SM 2 for new space station structure [J]. Robotics & Automation Magazine, IEEE, 1995, 2(4): 4-11.

[7] Fischer A, Pellegrino S. Interaction between gravity compensation suspension system and deployable structure [J]. Journal of Spacecraft and Rockets, 2000, 37(1): 93-99.